

Weierstraß-Institut
für Angewandte Analysis und Stochastik
Leibniz-Institut im Forschungsverbund Berlin e. V.

Preprint

ISSN 2198-5855

**A fully adaptive interpolated stochastic sampling method
for random PDEs**

Felix Anker, Christian Bayer, Martin Eigel,

Johannes Neumann, John Schoenmakers

submitted: December 21, 2015 (revision: January 11, 2017)

Weierstrass Institute
Mohrenstr. 39
10117 Berlin, Germany
E-Mail: felix.anker@wias-berlin.de
christian.bayer@wias-berlin.de
martin.eigel@wias-berlin.de
johannes.neumann@wias-berlin.de
john.schoenmakers@wias-berlin.de

No. 2200
Berlin 2015



2010 *Mathematics Subject Classification.* 35R60, 47B80, 60H35, 65C20, 65N12, 65N22, 65J10, 65C05 .

Key words and phrases. random PDE, stochastic differential equation, Feynman-Kac, interpolation, finite element, a posteriori error estimator, adaptive method, Euler Maruyama.

Edited by
Weierstraß-Institut für Angewandte Analysis und Stochastik (WIAS)
Leibniz-Institut im Forschungsverbund Berlin e. V.
Mohrenstraße 39
10117 Berlin
Germany

Fax: +49 30 20372-303
E-Mail: preprint@wias-berlin.de
World Wide Web: <http://www.wias-berlin.de/>

Abstract

A numerical method for the fully adaptive sampling and interpolation of PDE with random data is presented. It is based on the idea that the solution of the PDE with stochastic data can be represented as conditional expectation of a functional of a corresponding stochastic differential equation (SDE). The physical domain is decomposed by a non-uniform grid and a classical Euler scheme is employed to approximately solve the SDE at grid vertices. Interpolation with a conforming finite element basis is employed to reconstruct a global solution of the problem. An a posteriori error estimator is introduced which provides a measure of the different error contributions. This facilitates the formulation of an adaptive algorithm to control the overall error by either reducing the stochastic error by locally evaluating more samples, or the approximation error by locally refining the underlying mesh. Numerical examples illustrate the performance of the presented novel method.

1 Introduction

It becomes increasingly common that problems in the applied sciences, e.g. in engineering and computational biology, involve uncertainties of model parameters. These can for instance be related to coefficients of random media, i.e. material properties, inexact domains and stochastic boundary data. The uncertainties may result from heterogeneities and incomplete knowledge or inherent stochasticity of parameters. With steadily increasing computing power, the research field of uncertainty quantification (UQ) has become a rapidly growing and vividly active area of research which covers many aspects of dealing with such uncertainties for problems of practical interest.

In this work, we derive a novel adaptive numerical approach for the solution of PDEs with stochastic data. The proposed method is based on the presentation in [1] where a similar idea was described in combination with a global regression and without adaptivity (except for the step width in the Euler scheme). The important topic of adaptivity is picked up in this work where a *unique feature of the method is exploited*, namely the completely decoupled and localized parametrization (and thus control) of approximation errors and stochastic errors. This becomes feasible since

- the pointwise solution in the physical domain is determined by an appropriate SDE and solved by an adaptive Euler scheme as in [1],
- the global solution on the physical domain is reconstructed based on a triangulation and interpolation in between vertices (i.e. on a discrete finite element space).

Consequently, the overall error is determined by

- (i) the accuracy of the single SDE solutions determined by the step width of the scheme,
- (ii) the stochastic error for the pointwise expected value determined by the number of solutions computed on each vertex,

- (iii) the number of solution points in the physical domain determined by the refinement level of the employed mesh.

Hence, the second item related to the stochastic error enables a localized adaptivity for the sampling while the first and third items are related to the approximation quality in the physical domain. In comparison to other common methods such as the Monte Carlo FEM for stochastic PDEs [7], the proposed method provides means to *adjust the number of samples locally* while also reconstructing global solutions. Moreover, it is also highly parallelizable and thus well suited for modern distributed multi-core architectures.

While the derivation of the method in the next section is rather general, a specific motivation is given by a model relevant in practical problems, namely the Darcy equation related to the modeling of groundwater flow. It reads

$$\begin{aligned} (1a) \quad & -\nabla \cdot (\kappa(x)\nabla u(x)) = f(x), \quad x \in D, \\ (1b) \quad & u(x) = g(x), \quad x \in \partial D, \end{aligned}$$

where the solution u is the hydraulic head, κ denotes the conductivity coefficient describing the porosity of the medium, f is a source term and the Dirichlet boundary data is defined by g . The computational domain in d dimensions is denoted $D \subset \mathbb{R}^d$ and we suppose that D is a convex polygon. Moreover, all data are supposed to be sufficiently smooth such that the problem always exhibits a unique solution which then is also smooth. A detailed regularity analysis is not in the scope of this paper. In principle, although we restrict our investigations to a stochastic coefficient κ , any data of the PDE can be modeled as being stochastic. The model (1) is quite popular for analytical and numerical examinations since it is one of the simplest models which reveals some major difficulties that also arise in more complex stochastic models. Moreover, the deterministic second order elliptic PDE is a well-studied model problem and it is of practical relevance, e.g. in the context of groundwater contamination.

The stochastic data used in the PDE model is a stochastic field given with an adequate representation. This can for instance be based on actual measurements, expert-knowledge or simplifying assumptions regarding the statistics. For numerical computations, the representation has to be amenable for the employed method. It is a common modeling assumption that the random fields are Gaussian. They are then completely specified by the first two moments. In fact, any stochastic field $\kappa : \Omega \times D \rightarrow \mathbb{R}$ with finite variance can be represented by an expansion of the form

$$(2) \quad \kappa(x, \omega) = E[\kappa] + \sum_{m=1}^{\infty} a_m(x)\xi_m(\omega),$$

where the product in the sum separates the dependence on $\omega \in \Omega$ (a random event) and $x \in D$ (a point in the physical domain) with spatial functions a_m and independent random variables ξ_m . A typical approach to obtain such a representation is the Karhunen-Loève expansion (KL) which will be used in the numerical examples with a finite number of terms (truncated KL) [14, 19]. In this case, the basis a_m consists of eigenfunctions of the covariance integral operator weighted by the eigenvalues of this operator. The smoothness of the a_m is directly related to the smoothness of the covariance function used to model the respective stochastic field, see e.g. [8, 26, 19].

A variety of numerical methods is available to obtain approximate solutions of the model problem (1) with random data and we only refer to [19, 25, 18] for an overview in the context of uncertainty quantification (UQ). These methods often rely on the separation of the deterministic and the stochastic space and introduce separate discretizations [24]. Common methods are based on sampling of the stochastic space, the projection onto an appropriate stochastic basis or a perturbation analysis. The best known sampling approach is the Monte Carlo (MC) method which is very robust and easy to implement. Recent developments include the quite successful application of multilevel ideas for variance reduction and advances with structured point sequences (Quasi-MC), cf. [7, 9, 16, 17, 5]. (Pseudo-)Spectral methods represent a popular class of projection techniques which can e.g. be based on interpolation (Stochastic Collocation) [2, 22, 23] or orthogonal projections with respect to the energy norm induced by the differential operator of the random PDE (Stochastic Galerkin FEM) [14, 20, 4, 3, 13, 11, 12]. These methods are more involved to analyze and implement but offer the benefit of possibly drastically improved convergence rates when compared to standard Monte Carlo sampling. The deterministic discretization often relies on the finite element method (FEM) which also is employed with MC.

The aim of this paper is the description of a novel highly adaptive numerical approach which is founded on the observation that the random PDE (1) is directly related to a stochastic differential equation driven by a stochastic process, namely

$$(3) \quad dX_t = b(X_t) dt + \sigma(X_t) dW_t,$$

with appropriate coefficients b and σ , Brownian motion W and additional boundary conditions. For deterministic data κ, f, g , for any $x \in D$, the Feynman-Kac formula leads to a collection of random variables $\varphi^x = \varphi^x(\kappa, f, g)$ such that $u(x) = E[\varphi^x]$, i.e. the deterministic solution at x is equivalent to the expectation of the random variable. When the data are stochastic, the solution $u(\omega, x)$ of the random PDE at $x \in D$ can be expressed as the *conditional expectation* of u given data κ, f, g , i.e., $u(\omega, x) = E[\varphi^x | \kappa, f, g]$, and the variance of $u(x)$ can be bounded by the variance of φ^x . To determine φ^x at points $x \in D$, a classical Euler method can be employed. In order to recover a global solution in the physical domain D , opposite to the previous work [1] where global regression was utilized, we here rely on a mesh \mathcal{T} which is a regular triangulation of D . Sampled approximations of φ^x are then computed at the nodes of the mesh and the values are used for an interpolation in a discrete finite element space. This yields the approximate expectation of the solution $E[u(\omega, \cdot)]$ defined on the entire domain D .

A distinct advantage of this approach is the separation of all error components as mentioned above, which in the case of the discrete interpolation allows for the application of simple finite element (FE) a posteriori error estimates to refine the spatial mesh, i.e. the location of sample points in the domain guided by the global approximation error.

One can regard the proposed method as a combination of sampling and interpolation techniques, that make use of classical stochastic solution techniques pointwise and a global interpolation with FE basis functions. When compared to MC which samples a stochastic space (Ω, \mathcal{F}, P) by (typically) determining a FE solution at every point and subsequently averaging the solutions, our method determines realizations of stochastic solutions at points in the physical domain D and determines an approximation of the expectation by a global interpolation in the physical space. Thus, the method does not require any type of global deterministic solver and can be parallelized extremely well.

The structure of the paper is as follows: In Section 2, we elaborate on the representation of deterministic and stochastic PDEs in terms of stochastic differential equations (SDEs). Moreover, we recall the employed numerical methods to determine pointwise stochastic solutions, namely the Euler method and Monte Carlo sampling. Additionally, based on a deterministically chosen set of stochastic solutions in the physical domain, the reconstruction of a global approximation by means of an interpolation in a discrete FE basis is described. This allows for a fully adaptive algorithm which is derived in Section 3. There, the different error components are identified and a practical approach for the determination of the discretization parameters is explained. The paper is concluded with several numerical examples in Section 4 where the performance of the new method is demonstrated.

2 Stochastic Sampling and Interpolation

In this section we give a very short overview of the method presented in [1]. To give a very rough idea, we want to construct an SDE such that the solution $u(\omega, x)$ of the SPDE at some point $x \in D$ can be expressed as conditional expectation of some functional of the solution of an appropriate SDE. This forms the basis of the method which will be extended to a fully adaptive scheme.

For the sake of concreteness, we will present the method specifically in the case of Darcy's law and refer once more to [1] for the general form. For a more comprehensive treatment of the well-known basic stochastic theory, we refer for instance to [21].

2.1 Stochastic representations of PDEs

The starting point is the following SDE

$$(4a) \quad dX_t = \nabla \kappa(X_t) dt + \sqrt{2\kappa(X_t)} dW_t, \quad X_0 = x,$$

where $x \in D \subset \mathbb{R}^d$ is a deterministic point, W is a d -dimensional standard Brownian motion defined on some probability space (Ω, \mathcal{F}, P) and $\kappa : \Omega \times D \rightarrow \mathbb{R}$ is the *stochastic* field of conductivity coefficients associated to the medium. Furthermore, it is important to require the stochastic field κ and the Brownian motion W to be independent.¹

$$(4b) \quad Z_t := \int_0^t f(X_s) ds,$$

for the (again, possibly random, but independent from W) source term $f : \Omega \times D \rightarrow \mathbb{R}$. If we want to stress the dependence on the initial value, we write $X_t^x := X_t$. The process Z depends on x as well and we shall write Z_t^x if we want to stress this dependence. Notice that existence and uniqueness of solutions to the SDE can be obtained simply by applying standard theory after conditioning on the random fields κ and f , provided that the fields are regular enough.

¹This may require to enhance the original probability space Ω , on which κ is defined. See [1] for details.

In particular, we need to require that $\nabla \kappa$ exists and is Lipschitz continuous in x a.s. For more details on convenient regularity assumptions we once more refer to [1].

The (random) Dirichlet problem (1) now admits the following representation in terms of the solutions of the above SDE: Let $\tau = \tau_x$ denote the first hitting time of the solution $X = X^x$ (started at $x \in \overline{D}$) at the boundary ∂D . Then the random solution $u(x)$ and its expectation $E[u(x)]$ satisfy

$$(5) \quad u(x) = E \left[g \left(X_{\tau_x}^x \right) + Z_{\tau_x}^x \mid \kappa, f \right], \quad E[u(x)] = E \left[g \left(X_{\tau_x}^x \right) + Z_{\tau_x}^x \right].$$

This means that the random solution $u(x)$ is obtained from the random variable $g \left(X_{\tau_x}^x \right) + Z_{\tau_x}^x$ by taking expectations only w.r.t. the Brownian motion W . On the other hand, for $E[u(x)]$, we simply take the total expectation as there is no need for iterating the expectations.

Hence, for any $x \in D$ for which we want to obtain the solution $E[u(x)]$ of (1), we have to compute a solution of the SDE (4). We thus have to solve two problems,

- (i) Find an approximation \overline{X}_N of X_t , which is actually computable.
- (ii) Given such an approximation, the sought solution $E \left[g \left(\overline{X}_{\overline{\tau}} + \overline{Z}_{\overline{\tau}} \right) \right]$ is computed by a (quasi) Monte Carlo method, where over-lined expressions denote computable approximations.

2.2 Discretization of the SDE

Clearly the most popular approximation method for SDEs is a straight-forward generalization of the Euler method for ODEs. Indeed, let $0 = t_0 < \dots < t_N = t$ be a time grid, set

$$\Delta t_i := t_i - t_{i-1}, \quad \Delta W_i := W_{t_i} - W_{t_{i-1}}, \quad \Delta t_{\max} := \max_i \Delta t_i, \quad \overline{X}_0 := x,$$

and iteratively define

$$(6) \quad \overline{X}_i := \overline{X}_{i-1} + b \left(\overline{X}_{i-1} \right) \Delta t_i + \sigma \left(\overline{X}_{i-1} \right) \Delta W_i, \quad i = 1, \dots, N.$$

Under very weak assumptions we have *strong* convergence with rate 1/2, i.e.,

$$E \left[|X_t - \overline{X}_N| \right] \leq C \sqrt{\Delta t_{\max}}$$

for some constant C independent of Δt_{\max} . More relevant in most applications is the concept of *weak* approximation. Fortunately, the Euler scheme typically exhibits first order weak convergence, i.e., for any suitable test function $F : \mathbb{R}^d \rightarrow \mathbb{R}$, it holds

$$(7) \quad \left| E[F(X_t)] - E[F(\overline{X}_N)] \right| \leq C \Delta t_{\max}$$

with a constant C independent of Δt_{\max} for fixed times t . However, the stochastic representation (5) involves the process stopped at the first hitting time of the boundary ∂D of the domain. This stopping time is approximated by the first exit time $\overline{\tau}$ of the discrete time process \overline{X}_i , $i = 0, \dots, N$.

Note that there are two sources of errors in the approximation $\overline{X}_{\overline{\tau}}$ of X_{τ} :

- (i) the error in the approximation of X by \bar{X}
- (ii) the possibility that exit of X occurs between two grid points t_i and t_{i+1} while \bar{X} does not exit—or vice versa.

Indeed, even if two paths X and \bar{X} are close in, say, uniform norm, their exit times can be substantially different. Hence, the second source of error reduces the weak error rate, i.e., the approximation error for $E[u(x)]$ decreases to the rate $1/2$. For adaptive time-step refinements which can recover the order of convergence to an observed order 1 again, we refer to the references given in [1].

2.3 Monte Carlo approximation of the expectation

Another step in the discretization is the approximation of the expected value as in (5) with a Monte Carlo estimator. Multilevel Monte Carlo methods are also possible but require the construction of two related realizations of \bar{X}_M for each sample on the individual levels as described in [15]. Here, we restrict ourselves to the classical Monte Carlo estimator which is defined as

$$(8) \quad \mathbb{E}_{M,N}^{\text{MS}}[u(x)] := \frac{1}{N} \sum_{i=1}^N g(\bar{X}_{\bar{\tau}}^x(\omega_i)) + \bar{Z}_{\bar{\tau}}^x(\omega_i),$$

where $(\omega_i)_{i=1}^N$ is a set of $N \in \mathbb{N}$ samples drawn from the probability space $(\Omega, \mathcal{F}, \mathbb{P})$ and M describes the number of steps for the discrete diffusion process. Note that this random space represents both the Brownian motion W and the random field κ from the initial Darcy problem (1). Recall that

$$\bar{Z}_{\bar{\tau}}^x = \int_0^{\bar{\tau}} f(X_s) \, ds,$$

which we approximate by a simple left-point rule $\bar{Z}_{\bar{\tau}}$. Hence,

$$\begin{aligned} \bar{X}_0 &= x, \\ \bar{X}_m &= \bar{X}_{m-1} + \nabla \kappa(\bar{X}_{m-1}) \Delta t_m + \sqrt{2\kappa(\bar{X}_{m-1}) \Delta t_m} \mathcal{N}_{0,1}, \end{aligned}$$

where M is the last index with $\bar{X}_m \in D$ for $m = 0, \dots, M$ and $\bar{X}_{M+1} \notin D$. Here, $\mathcal{N}_{0,1}$ denotes the standard normal distribution in d dimensions. The stopping position and the stopping time $t_{\bar{\tau}}$ of the diffusion process is now approximated by the projection

$$(9) \quad \bar{X}_{\bar{\tau}} := \arg \min \{ \|x - \bar{X}_M\| \mid x \in \partial D, x = \bar{X}_M + s(\bar{X}_{M+1} - \bar{X}_M), s \geq 0 \}$$

of \bar{X}_M onto the boundary ∂D in direction of \bar{X}_{M+1} . (8) provides the estimator with a simple one-point integration rule via

$$\mathbb{E}_{M,N}^{\text{MS}}[u(x)] := \frac{1}{N} \sum_{i=1}^N \left(g(\bar{X}_{\bar{\tau}}(\omega_i)) + \sum_{m \in (0, \dots, M, \bar{\tau})} f(\bar{X}_m(\omega_i)) \Delta t_m \right).$$

Simple time adaptivity is applied by choosing $\Delta t_j = \text{dist}(\partial D, \bar{X}_{j-1})\Delta t_0$ where $\text{dist}(\partial D, x) := \min \{\|x_d - x\| \mid x_d \in \partial D\}$ is the Euclidean distance to the boundary of the domain. The entire process is depicted in Algorithm 1 where a simple rectangle integration method is used. Moreover, Figure 1 sketches the described process.

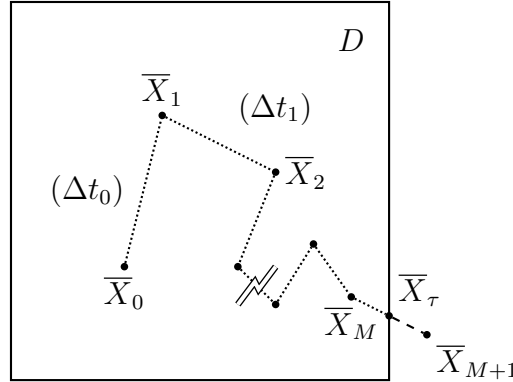


Figure 1: Sketch of a discrete diffusion process realization with endpoint projection and indicated step width.

In : point $x \in D$, number of samples N , initial time step Δt_0

Out: $E_{M,N}^{\text{MS}}[u(x)]$

```

for  $i = 0, \dots, N$  do
   $\bar{X}_0 = x$ 
   $F = 0$ 
   $m = 1$ 
  sample  $\kappa^i = \kappa(\omega_i)$  with  $\omega_i \in \Omega$ 
  while  $\bar{X}_m \in D$  do
     $F = F + f(\bar{X}_{m-1})\Delta t_{m-1}$ 
     $\Delta t_m = \min \{ \text{dist}(\partial D, \bar{X}), 1 \} \Delta t_0$ 
    sample  $\Xi$  from  $\mathcal{N}_{0,1}$ 
     $\bar{X}_m = \bar{X}_{m-1} + \nabla \kappa^i(\bar{X}_{m-1})\Delta t_m + \sqrt{2\kappa^i(\bar{X}_{m-1})\Delta t_m}\Xi$ 
     $m = m + 1$ 
  compute  $\bar{X}_\tau$  and  $t_\tau$  according to (9)
   $F = F + f(\bar{X}_\tau)\Delta t_\tau$ 
   $u^i = g(\bar{X}_\tau) + F$ 
return  $N^{-1} \sum_{i=0}^N u^i$ 

```

Algorithm 1: Point estimate algorithm to compute the estimator $E_{M,N}^{\text{MS}}[u(x)]$ using the simple one-point rectangle method for integration.

2.4 Extension to the whole Domain

In the following, the pointwise approximation of the solution at some $x \in D$ obtained by some Monte Carlo estimator is extended to the whole domain D using interpolation techniques on a mesh. This allows to apply finite element a posteriori error control with respect to a global (in D) approximation of the solution which we define as follows: Consider some given mesh \mathcal{T}_h as a triangulation of the physical domain D with vertices $\mathcal{N}_h = (\nu_h^i)_{i=1}^{|\mathcal{N}_h|}$ and edges $\mathcal{E}_h = \{E_i\}_{i=1}^{|\mathcal{E}_h|}$. Note that the coefficients of a Courant P_1 function correspond to the function values at the vertices (nodes) of the mesh and that the nodal interpolation operator denoted by \mathcal{I}_h is defined by these values. Hence, let the discrete solution $\mathbf{E}_{\mathbf{M},\mathbf{N}}^{\text{MS}}[u_h]$ with $\mathbf{M} = (M_i)_{i=1}^{|\mathcal{N}_h|}$ and $\mathbf{N} = (N_i)_{i=1}^{|\mathcal{N}_h|}$ be a Courant P_1 function on this mesh determined by setting the nodal values,

$$\mathbf{E}_{\mathbf{M},\mathbf{N}}^{\text{MS}}[u_h](\nu_h^i) := \mathbf{E}_{M_i, N_i}^{\text{MS}}[u(\nu_h^i)] \quad \text{for } i = 1, \dots, |\mathcal{N}_h|.$$

This introduces three types of errors into the global approximation of u . The first is the *stochastic approximation error* originating from the Monte Carlo estimators. It can be controlled by means of the Central Limit Theorem (CLT) subject to the number of samples N_i for each nodal point. The second error arises from the *approximation of the diffusion process* and is controlled by the parameters M_i , i.e. the number of time steps. The third error contribution results from the P_1 *interpolation* which is approximated based on the Monte Carlo estimators and determined by the interpolation mesh parameter h .

We shall consider two error representations. The first describes a *decomposition of the mean square error* into three error parts resulting from the interpolation error, the discretization of the ordinary differential equation, and the sampling error in the Monte Carlo method. For this, define the expected value of the discrete ordinary differential equation as $\mathbf{E}[u_h^M] := \mathbf{E}[\mathbf{E}_{\mathbf{M},\mathbf{N}}^{\text{MS}}[u_h]]$. Then it holds for the pointwise mean square error in the approximation that

$$\begin{aligned} \mathbf{E}\left[\left(\mathbf{E}_{\mathbf{M},\mathbf{N}}^{\text{MS}}[u_h] - \mathbf{E}[u]\right)^2\right] &= \mathbf{E}\left[\mathbf{E}_{\mathbf{M},\mathbf{N}}^{\text{MS}}[u_h]^2\right] - 2\mathbf{E}\left[\left(\mathbf{E}_{\mathbf{M},\mathbf{N}}^{\text{MS}}[u_h]\right)\mathbf{E}[u]\right] + \mathbf{E}[u]^2 \\ (10) \quad &= \mathbf{E}\left[\mathbf{E}_{\mathbf{M},\mathbf{N}}^{\text{MS}}[u_h]^2\right] - \mathbf{E}[u_h^M]^2 + \left(\mathbf{E}[u_h^M] - \mathbf{E}[u]\right)^2 \\ &= \frac{1}{N} \text{Var}[u_h^M] + \left(\mathbf{E}[u_h^M] - \mathbf{E}[u]\right)^2. \end{aligned}$$

The second decomposition seeks to represent the error *locally in the L^2 norm*. We assume some convex $D \subseteq \mathbb{R}^2$ for the sake of a simpler presentation and H^2 regularity of the solution u . Higher dimensions are possible with different inequalities for the norms. Consider the element $T \in \mathcal{T}_h$ and the pointwise P_1 interpolation operator \mathcal{I}_h on the mesh \mathcal{T}_h . By a triangle inequality and interpolation error estimates, for the approximation error it holds

$$\begin{aligned} \|\mathbf{E}[u] - \mathbf{E}_{\mathbf{M},\mathbf{N}}^{\text{MS}}[u_h]\|_{L^2(T)} &\lesssim \|\mathbf{E}[u] - \mathcal{I}_h \mathbf{E}[u]\|_{L^2(T)} + \|\mathcal{I}_h \mathbf{E}[u] - \mathbf{E}_{\mathbf{M},\mathbf{N}}^{\text{MS}}[u_h]\|_{L^2(T)} \\ &\lesssim \|\mathbf{E}[u] - \mathbf{E}[u_h]\|_{L^2(T)} + \|\mathbf{E}[u_h] - \mathcal{I}_h \mathbf{E}[u]\|_{L^2(T)} \\ &\quad + \|\mathcal{I}_h \mathbf{E}[u] - \mathbf{E}[u_h^M]\|_{L^2(T)} + \|\mathbf{E}[u_h^M] - \mathbf{E}_{\mathbf{M},\mathbf{N}}^{\text{MS}}[u_h]\|_{L^2(T)} \\ (11) \quad &\lesssim h_T \eta_T + h_T^2 \|\Delta u\|_{L^2(T)} + |T| \Delta t_0 + |T| \max_{K \in \mathcal{N}(T)} \left\{ \text{Var}[u_h^M]^{1/2} N_K^{-1/2} \right\}. \end{aligned}$$

The element-wise error indicator η_T which controls the FE approximation error is described in Section 3. The first two terms are both governed by properties of the mesh \mathcal{T}_h and can be controlled through refinement as well as the adaptive algorithms described in Section 3. The third term represents the Monte Carlo estimation error. It solely depends on the number of samples used for each node in the element as the variance converges to the variance of the continuous solution $\text{Var}[u]$ for $M \rightarrow \infty$ and $h \rightarrow 0$. The last term represents the error in the approximation of the diffusion process in the Euler scheme for the stochastic differential equation. Numerical experiments show that $\Delta t_0 \simeq h_{\min}$ is a reasonable choice in the two-dimensional case.

3 Adaptivity

To achieve convergence of the method presented in Section 2 by means of an adaptive algorithm, all error components in the decomposition (11) have to converge separately. For optimal convergence, for all contributing parts the same rate should be achieved with respect to the computational effort that has to be invested to gain the error reduction. The main idea of an adaptive algorithm is therefore to base the parameter choices in some way on the underlying mesh. Hence, in the following it is the goal to define some optimal sequence of meshes $\mathcal{T}_0 \subset \dots \subset \mathcal{T}_L$ for the interpolation and then to choose appropriate values for the other discretization parameters.

We use the convenience notation $a \lesssim b$ (or $a \approx b$) to state that $a \leq Cb$ (or $C^{-1}b = a = Cb$) with a constant $C > 0$ independent of the discretization parameters.

Our starting point is an initial quasi-uniform triangulation \mathcal{T}_0 of the physical domain D . The first step is to calculate a discrete solution $E_{M_0, N_0}^{\text{MS}}[u_0]$. The parameters M_0 and N_0 have to be guessed as not enough information is available on the initial level². The next step involves the calculation of some finite element error indicator η_0 which we briefly describe.

One of the most common and simple a posteriori FE error estimation techniques is given by the residual error estimator. We define the local error indicator $\eta_{h,T}$ on some element $T \in \mathcal{T}_h$ of size h_T subject to an approximation u_h of the true solution u by

$$(12) \quad \eta_{h,T}^2 = h_T^2 \|f\|_{L^2(T)}^2 + \sum_{E \in \mathcal{E}(T)} h_T \|\nabla u_h \cdot n_E\|_{L^2(E)}^2.$$

Recall that the set of edges of \mathcal{T}_h is denoted \mathcal{E}_h and the edges of some element T are denoted $\mathcal{E}(T)$. More details and a proper derivation can e.g. be found in [6] and the references therein.

Once a local error indicator $\eta_{h,T}$ is readily available, a mesh refinement strategy can be chosen which selects a set of elements $\mathcal{M}_h \subset \mathcal{T}_h$ such that an error reduction is achieved for the approximate solution on the finer mesh. A common choice is the so-called bulk or Dörfler marking defined for some fraction parameter $0 < \theta \leq 1$ by

$$(13) \quad \sum_{T \in \mathcal{M}_h} E[\eta_{h,T}]^2 \geq \theta \sum_{T \in \mathcal{T}_h} E[\eta_{h,T}]^2.$$

²the subscript denotes the refinement level for which the parameters or functions are considered

We also employ this marking and refer to [10] for further details, in particular with regard to error reduction properties.

As can be seen in (11), the estimator only covers the first term $\|\mathbf{E}[u] - \mathbf{E}[u_0]\|_{L^2(T)}$ and thus the parameters M_0 and N_0 have to be chosen such that

$$h_T \eta_{0,T} \gg \|\mathcal{I}_h \mathbf{E}[u] - \mathbf{E}[u_h^M]\|_{L^2(T)} + |T| \max_{K \in \mathcal{N}(T)} \left\{ \text{Var}[u_h^M]^{1/2} N_K^{-1/2} \right\}.$$

The reason for this is that the finite element solution is bounded by the interpolator but the stochastic properties of the discrete solutions introduce oscillations of length h and amplitudes as seen above. These can be unbounded in principle and artificially increase the finite element error estimator. As refinement would not reduce these oscillations, we have to limit them by means of the central limit theorem such that we can get reliable mesh refinements. In fact, the stochastic error term from (11) for each element has to be smaller than the smallest error estimator $\eta_{\ell,T}$ chosen for the refinement set \mathcal{M}_ℓ (on refinement levels $\ell = 1, \dots, L$) given by

$$(14) \quad \min_{T \in \mathcal{M}_\ell} \eta_{0,T} > |T| \max_{K \in \mathcal{N}_\ell(T)} \left\{ \text{Var}[u_h^M]^{1/2} N_K^{-1/2} \right\} + \|\mathcal{I}_h \mathbf{E}[u] - \mathbf{E}[u_h^M]\|_{L^2(T)}.$$

This constraint also includes the error of the approximation in the Euler scheme but it is deterministic, smooth, and global with respect to the physical domain D . As a result, it alters the error estimator only to some minor extent.

The derived refinement \mathcal{T}_1 of the initial mesh \mathcal{T}_0 is the basis for the next level and the process is repeated. Heuristics based on educated guesses of the error components allow to balance the parameters in actual computations. This however is only possible if there are at least three meshes, that is $L \geq 3$. Section 3.1 covers some approaches to this topic in more detail.

3.1 A Practical Parameter Selection Strategy

The error decomposition in (11) results in three components that need to be balanced for guaranteed and optimal convergence. We hence aim at finding good estimates for the convergence rates with respect to the relevant parameters and then extrapolate the error estimates to the next level. With these, we can approximate parameters that fulfill the balancing requirements. The first task is the approximation of the convergence rate of the interpolation error subject to the current mesh and controlled through the parameter α . Let h be the minimal inradius over all the triangles of the triangulation \mathcal{T}_h and suppose we have some $\alpha > 0$ such that

$$\|\mathbf{E}[u] - \mathbf{E}[\mathcal{I}_h u]\|_{L^2(D)} \lesssim h^\alpha.$$

Standard finite element theory gives

$$\|\mathbf{E}[u] - \mathbf{E}[\mathcal{I}_h u]\|_{L^2(D)} \sim \|\mathbf{E}[u] - \mathbf{E}[u_h]\|_{L^2(D)}.$$

Thus, with some efficient and reliable error estimate $h\eta_h \sim \|\mathbf{E}[u] - \mathbf{E}[u_h]\|_{L^2(D)}$, we get $h\eta_h \sim h^\alpha$. We exploit this property to gauge the parameter α as error estimators have smoothing properties and thus in practice exhibit a behavior closer to a monotonic convergence. For the estimation α_L of α , we carry out a linear regression over data points $(\log(h_\ell), \log(h\eta_\ell))_{\ell=1, \dots, L}$.

Next, we estimate the expected spatial error on the next level $L + 1$. For this, the triangle inequality for $\ell = 1, \dots, L$ yields

$$\|\mathbf{E}[u] - \mathbf{E}[u_\ell]\|_{L^2(D)} \leq \|\mathbf{E}[u] - \mathbf{E}[u_L]\|_{L^2(D)} + \|\mathbf{E}[u_L] - \mathbf{E}[u_\ell]\|_{L^2(D)}.$$

The last term on the right-hand side is computable and it remains to estimate the error on level L . We assume $\|\mathbf{E}[u] - \mathbf{E}[u_L]\|_{L^2(D)} \ll \|\mathbf{E}[u_L] - \mathbf{E}[u_\ell]\|_{L^2(D)}$ for the coarser levels $\ell < L$ and thus conclude that

$$\|\mathbf{E}[u] - \mathbf{E}[u_\ell]\|_{L^2(D)} \approx \|\mathbf{E}[u_L] - \mathbf{E}[u_\ell]\|_{L^2(D)}$$

for each level $\ell = 1, \dots, L - 1$.

As we already have a good approximation of the expected convergence rate α_L , we can now find approximations of the error $\|\mathbf{E}[u] - \mathbf{E}[u_L]\|_{L^2(D)}$ with the help of the errors on the coarser levels by

$$\|\mathbf{E}[u] - \mathbf{E}[u_\ell]\|_{L^2(D)} \sim h_\ell^\alpha \quad \text{and} \quad \|\mathbf{E}[u] - \mathbf{E}[u_L]\|_{L^2(D)} \sim h_L^\alpha.$$

For each $\ell = 1, \dots, L - 1$, this asymptotically yields the identity

$$\frac{\|\mathbf{E}[u] - \mathbf{E}[u_L]\|_{L^2(D)}}{\|\mathbf{E}[u] - \mathbf{E}[u_\ell]\|_{L^2(D)}} = \frac{h_L^\alpha}{h_\ell^\alpha}.$$

Hence, we can construct the approximation

$$\|\mathbf{E}[u] - \mathbf{E}[u_L]\|_{L^2(D)} \approx \frac{h_L^\alpha}{h_\ell^\alpha} \|\mathbf{E}[u_L] - \mathbf{E}[u_\ell]\|_{L^2(D)}.$$

We subsequently define the estimate \tilde{e}_L for the error $\|\mathbf{E}[u] - \mathbf{E}[u_L]\|_{L^2(D)}$ on level L as the arithmetic mean of the different extrapolations from the coarser levels $\ell = 1, \dots, L - 1$ by

$$\tilde{e}_L := \frac{1}{L-1} \sum_{\ell=1}^{L-1} \frac{h_L^\alpha}{h_\ell^\alpha} \|\mathbf{E}[u_L] - \mathbf{E}[u_\ell]\|_{L^2(D)}.$$

The same technique is used to gauge the expected error on level $L + 1$. The finer mesh \mathcal{T}_{L+1} on level $\ell = L + 1$ is obtained from a local refinement (13). Thus, the parameter h_{L+1} can be used to generate the extrapolation \dot{e}_{L+1} with the same levels $L = 1, \dots, L - 1$,

$$\dot{e}_{L+1} := \frac{1}{L-1} \sum_{\ell=1}^{L-1} \frac{h_{L+1}^\alpha}{h_\ell^\alpha} \|\mathbf{E}[u_L] - \mathbf{E}[u_\ell]\|_{L^2(D)}.$$

The next step is to balance the expected Monte Carlo error with the extrapolated spatial error. For the refinement scheme (13), it is crucial to keep the Monte Carlo error well below the spatial error as otherwise this error gets picked up by the estimator which results in wrong refinement and thus unstable behavior and suboptimal convergence or even in no convergence

at all. Hence, we introduce the balancing factor δ which describes the desired relation between the two errors in (10) by

$$(15) \quad \delta^2 = \frac{(\mathbb{E}[u] - \mathbb{E}[u_h^M])^2}{N^{-1} \text{Var}[u_h^M]}.$$

A choice of $\delta = 1$ would lead to equality. For some constant c_N^ℓ for each level $\ell = 1, \dots, L$, we set the numbers of samples in the vertices $\mathcal{N}_\ell = (\nu_\ell^i)_{i=1}^{|\mathcal{N}_\ell|}$ as

$$(16) \quad N_\ell^i := c_N^\ell \text{Var}[u_\ell^M(\nu_\ell^i)] \quad \text{for } i = 1, \dots, |\mathcal{N}_\ell|.$$

The next task is to choose c_N^{L+1} appropriately so that (15) will be fulfilled for $h = h_{L+1}$. In fact, applying (16) to (15) results in

$$\mathbb{E}[u] - \mathbb{E}[u_L^M] = \delta (c_N^L \text{Var}[u_L^M])^{-1/2} \text{Var}[u_L^M]^{1/2}.$$

We assume $\text{Var}[u_\ell^M] \approx \text{Var}[u^M]$ for $\ell = 1, \dots, L$ is a sufficient approximation since only a rough estimate of the variance is needed. Taking the L^2 norm of the last equation and applying the variance approximation yields

$$c_N^L = \frac{|D|^2}{\delta^2} \|\mathbb{E}[u_L^M] - \mathbb{E}[u]\|_{L^2(D)}^{-2}.$$

With the extrapolated estimate $\dot{e}_{L+1} \approx \|\mathbb{E}[u] - \mathbb{E}[u_{L+1}^M]\|$, we get an estimate for the constant c_N^{L+1} as $\dot{c}_N^{L+1} = \frac{|D|^2}{\delta^2} \dot{e}_{L+1}^{-2}$. The numbers of samples for level $L + 1$ are now set according to (16) by

$$(17) \quad N_{L+1}^i := \dot{c}_N^{L+1} \text{Var}[u_L^M(\nu_{L+1}^i)] \quad \text{for } i = 1, \dots, |\mathcal{N}_{L+1}|.$$

Remark 3.1. It is imperative to ensure a minimum number of samples for each N_L^i in (17) since on each level a sufficient approximation of the variance $\text{Var}[u_\ell^M]$ has to be available. This is important since otherwise the algorithm might become unstable due to severe undersampling in single points. This would result in a bad spatial error estimation in (14) and thus suboptimal mesh refinement with reduced convergence rate or even lack of convergence.

To alleviate this issue, a simple solution is to choose some N_{\min} independent of all parameters and especially independent of the level ℓ . The practical application requires some rough estimate of the variance which can be computed alongside the expected value and thus set the numbers of samples on level $L + 1$ as

$$(18) \quad \dot{N}_{L+1}^i := \max \left\{ \dot{c}_N^{L+1} \text{Var}_{M,N}^{\text{MC}}[u_L^M(\nu_{L+1}^i)], N_{\min} \right\} \quad \text{for } i = 1, \dots, |\mathcal{N}_{L+1}|.$$

Finally, it remains to choose the parameter Δt on each level. The influence of this parameter on the error is given in the last term of (11). Since we assume linear pointwise convergence with respect to Δt , we choose the relation $h \sim \Delta t$. In Algorithm 2, the overall adaptive algorithm is sketched. The computation of the employed pointwise solution estimator $\mathbb{E}_{M,N}^{\text{MS}}[u_\ell]$ is depicted in Algorithm 1.

Note that instead of the variance based adaptive local number of samples for each vertex, one could also choose a common number of samples based on the variance $\text{Var}[u_L^M]$.

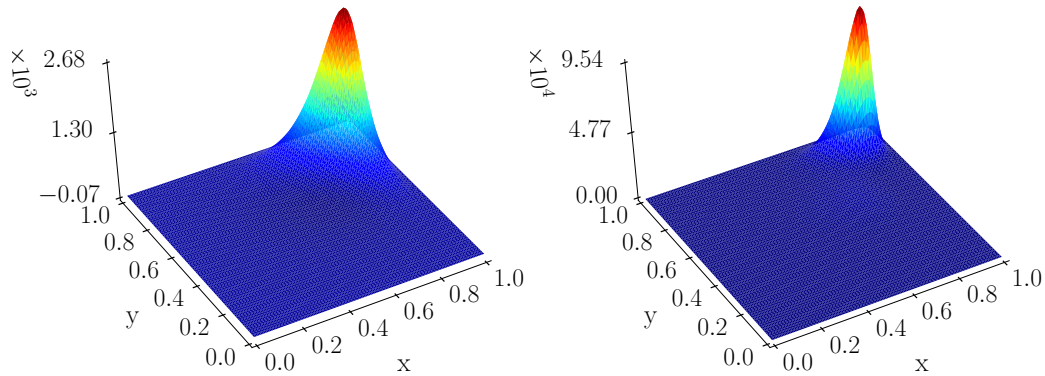


Figure 2: The mean (left) and the variance (right) of the solution for the numerical example.

Remark 3.2. In the numerical calculations one has to impose (14) well enough, such that the algorithm becomes stable. This can be achieved by choosing $\delta < 1$. In the experiments in Section 4, we choose $\delta = 0.2$. This allows for a stable algorithm and only imposes a slight impact on performance.

3.2 Adaptation to a Goal Functional

Additionally to the global solution we consider the computation of a derived quantity of interest of the form

$$(19) \quad Q(u) = \mathbb{E} \left[\int_D g u \, dx \right].$$

In the case when the support of g is smaller than D we can restrict the computations to that subdomain. In the general case however it is easier and even more efficient to adapt the heuristics to cater for the different error contributions with respect to the quantity of interest. To facilitate this we introduce the defining function g as a weight in the heuristics for the mesh refinement in (12) and for the number of samples in (17). Instead of $\eta_{h,T}$ from (12) we consider

$$\eta_{h,t,g}^2 := h_T^2 \|gf\|_{L^2(T)}^2 + \sum_{E \in \mathcal{E}(T)} h_T \|g \nabla u_h \cdot n_E\|_{L^2(E)}^2.$$

for the mesh refinement indicator. For the number of samples we weight the estimator similarly such that instead of \dot{N}_{L+1}^i in (18) we apply

$$\dot{N}_{L+1}^i := \max \{ g(x_i) \hat{g}^{-1} c_N^{L+1} \text{Var}_{\mathbf{M}, \mathbf{N}}^{\text{MC}} [u_L^M(\nu_{L+1}^i)], N_{\min} \} \quad \text{for } i = 1, \dots, |\mathcal{N}_{L+1}|.$$

where \hat{g} is the maximum of g in the domain D and x_i is the location of vertex i .

4 Numerical Experiments

This section is concerned with the illustration of the presented adaptive sampling method based on some numerical benchmark problems. The visualizations show properties of the unique feature of this approach, namely its proper separation of the physical and stochastic domain. This

In : $\mathcal{T}_0, N_{init}, \Delta t_0$

Out: solution $E_{M,N}^{MS}[u_L]$

```

for  $\ell = 1, \dots, L$  do
  if  $\ell \geq 2$  then
    | compute  $N_\ell$  according to (18)
  else
    | set  $N_\ell$  to  $N_0$ 
  set  $\Delta t$  according to  $h$ 
  compute  $E_{M,N_\ell}^{MS}[u_\ell]$  and  $\text{Var}_{M,N_\ell}^{MS}[u_\ell]$  at  $x \in \mathcal{N}_\ell$  with Algorithm 1
  if  $\ell = L$  then
    | break
  compute  $\eta_\ell$ 
  refine  $\mathcal{T}_\ell$  with  $\eta_\ell$  to get  $\mathcal{T}_{\ell+1}$ 
return  $E_{M,N}^{MS}[u_L]$ 

```

Algorithm 2: Adaptive Algorithm for the stochastic representation.

allows to choose the number of samples locally based on the variance in any part of the physical domain as well as to exploit sparsity with respect to the sampling locations. For comparison purposes we compute the solution for the experiments with a fixed number of samples for all the nodal points in the domain using uniform and adaptive meshes and we use different numbers of samples for the same meshes.

Consider the input data $f = \Delta u^*$ with

$$u^* = 5x^2(1-x)^2(e^{10x^2} - 1)y^2(1-y)^2(e^{10y^2} - 1)$$

together with the random field

$$\kappa(x) = \frac{c_a}{\alpha_{\min}} \left(\sum_{m=1}^{t_a} a_m(x) \varphi_m + \alpha_{\min} \right) + \varepsilon_a.$$

Here, the φ_m are uniformly distributed independent random variables. The parameters $c_a, \varepsilon_a > 0$ and the truncation length $t_a \in \mathbb{N}$ control the properties of the random field. The coefficients a_m are defined for $m = 1, 2, \dots$ for the parameters $\sigma_\alpha > 1$ and $0 < A_\alpha < 1/\zeta(\sigma_\alpha)$ with the Riemann zeta function ζ by

$$\begin{aligned} a_m(x) &= \alpha_m \cos(2\pi\beta_1(m)x_1) \cos(2\pi\beta_2(m)x_2), \quad \alpha_m = A_\alpha m^{-\sigma_\alpha}, \\ \beta_1(m) &= m - k(m)(k(m) + 1)/2, \quad \beta_2(m) = k(m) - \beta_1(m), \\ k(m) &= \lfloor -1/2 + \sqrt{1/4 + 2m} \rfloor. \end{aligned}$$

In our experiment we choose the setting $\sigma_\alpha = 2, A_\alpha = 0.6, c_\kappa = 1, \varepsilon_\alpha = 0.5 \cdot 10^{-3}$ and $t_\alpha = 5$. Together with the prescribed right-hand side f this results in strong oscillations in the corner $(1, 1)$ of the unit square together with a high variance of the solution in the same

region. The resulting mean $E[u]$ and variance $\text{Var}[u]$ are depicted in Figure 2 as computed by a standard Monte Carlo finite element method.

The algorithm automatically chooses the number of samples locally and applies mesh adaptivity at the same time. Plotting the numbers of samples for each vertex of the mesh as a P_1 projection thus gives a false impression of the distribution of the computational effort in the physical domain. Hence, we define the additional quantity

$$(20) \quad \mathcal{C}_T = \frac{1}{3|T|} \sum_{i=1}^3 N_i$$

which gives the average number of samples used for each element weighted by the size of that element as a measure for the computational error per area.

In the experiments we set the minimum number of samples N_{\min} for each vertex as 100. We continue the algorithm until our error heuristic drops below the prescribed value $\|e^{\text{MS}}\|_{H^1} = \|E[u] - E_{M,N}^{\text{MS}}[u_h]\|_{H^1} \leq 2 \cdot 10^3$. We consider four experiments. The first uses a fixed number of samples for each level and uniform meshes, the second one applies adaptive meshes, the third experiment combines uniform meshes with locally chosen numbers of samples, and the fourth experiment uses both adaptive meshes and local sample adaptivity.

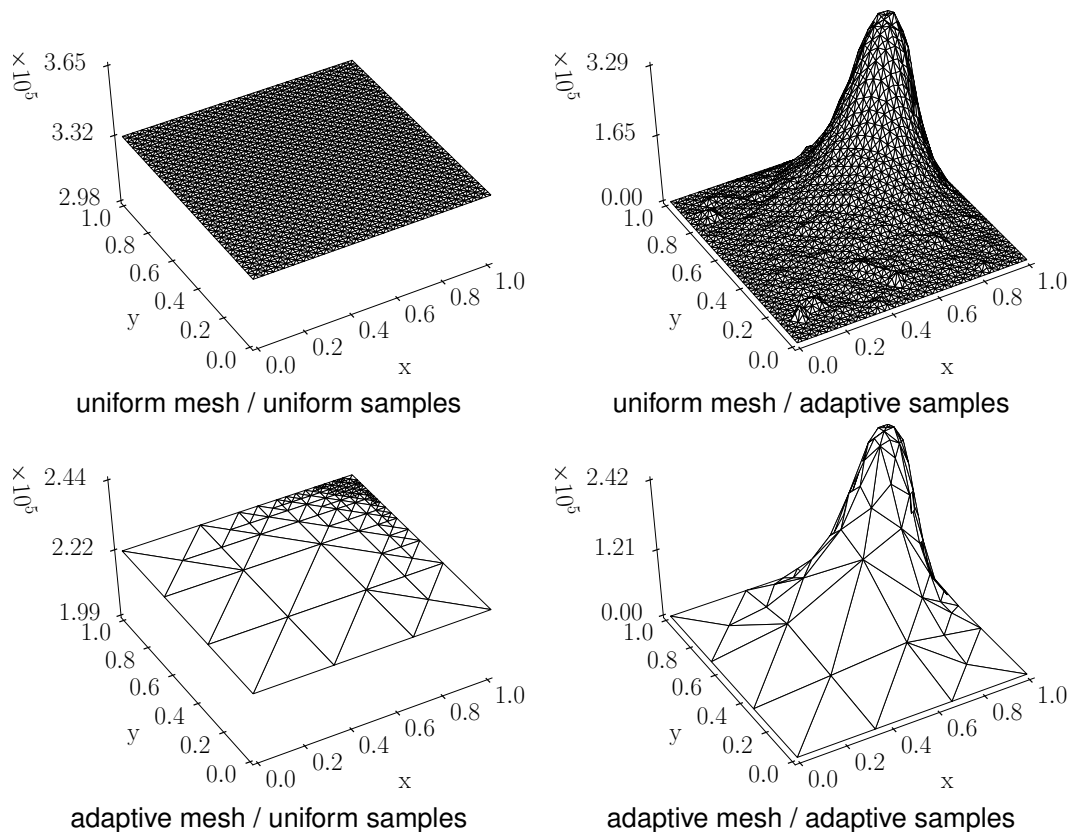


Figure 3: The number of samples for each vertex for different methods.

The resulting numbers of samples are plotted in Figure 3. Note that already a computational advantage is visible for the adaptive sampling variants whereas both uniform sampling experi-

ments falsely appear to be similar in effort. This changes if one considers the plots of \mathcal{C}_T shown in Figure 4. The adaptive mesh reduces the amount of vertices in the smooth regions of the solution whereas the local sample number reduces the number of samples for vertices with a small variance. In the optimal case of the combined method, the adaptivity eliminates a lot of expensive vertices with a high number of samples and the local sampling reduces the number of samples in areas with a highly oscillating mean.

The maximum computational effort is in the same order of magnitude for all four experiments but the computational effort \mathcal{C}_T drops dramatically away from the $(1, 1)$ -corner in all but the first experiment. This effect is more pronounced for the two experiments with mesh adaptivity. The last experiment improves this even further as fewer samples are used for the small triangles which are closer to $(0.5, 1)$ and $(1, 0.5)$.

The above observations correspond with the convergence in the H^1 norm with respect to the measured processor time as presented in Figure 5. The slowest method uses uniform meshes and applies a constant number of samples for all vertices in the domain. Local numbers of samples reduce the time almost nine-fold whereas the mesh adaptivity gives an improvement factor of 80. The combination of the two methods gives the fastest algorithm with an increase in speed of almost two orders of magnitude.

In Figure 6 the convergence of the error in the L^2 norm is plotted with respect to the same computational effort. Here again, a uniform mesh with constant sample numbers results in the slowest method. Contrary to the last graph, all other methods perform very similarly to each other with an approximate improvement of 8-10 compared to the slowest approach.

In the final example we consider the weight for the goal functional in (19)

$$g = \begin{cases} C_g \varepsilon_g^{-2} \exp\left(\frac{-1}{1 - \|x_0 - x\|^2 \varepsilon_g^{-2}}\right) & \text{if } \|x_0 - x\| \leq \varepsilon, \\ 0 & \text{else.} \end{cases}$$

We choose the location $x_0 = [0.6, 0.8]$, radius $\varepsilon_g = 0.1$, and weight $C_g = 2.14$. In Figure 7 the effect of the different adaptive methods is shown. The greatest benefit stems from the goal-weighted adaptive finite element method by comparing uniform methods with global adaptivity as in the previous example and the goal-weighted adaptive methods. Compared to uniform refinements it is up to two orders of magnitude faster in achieving the same error level. Local adaptive variance and its goal-weighted variant add upon this improvement. With global finite element adaptivity no convergence with respect to the goal is observed.

References

- [1] Felix Anker, Christian Bayer, Martin Eigel, Marcel Ladkau, Johannes Neumann, and John Schoenmakers. SDE based regression for random PDEs. *WIAS preprint*, 2015.
- [2] Ivo Babuška, Fabio Nobile, and Raúl Tempone. A stochastic collocation method for elliptic partial differential equations with random input data. *SIAM J. Numer. Anal.*, 45(3):1005–1034, 2007.

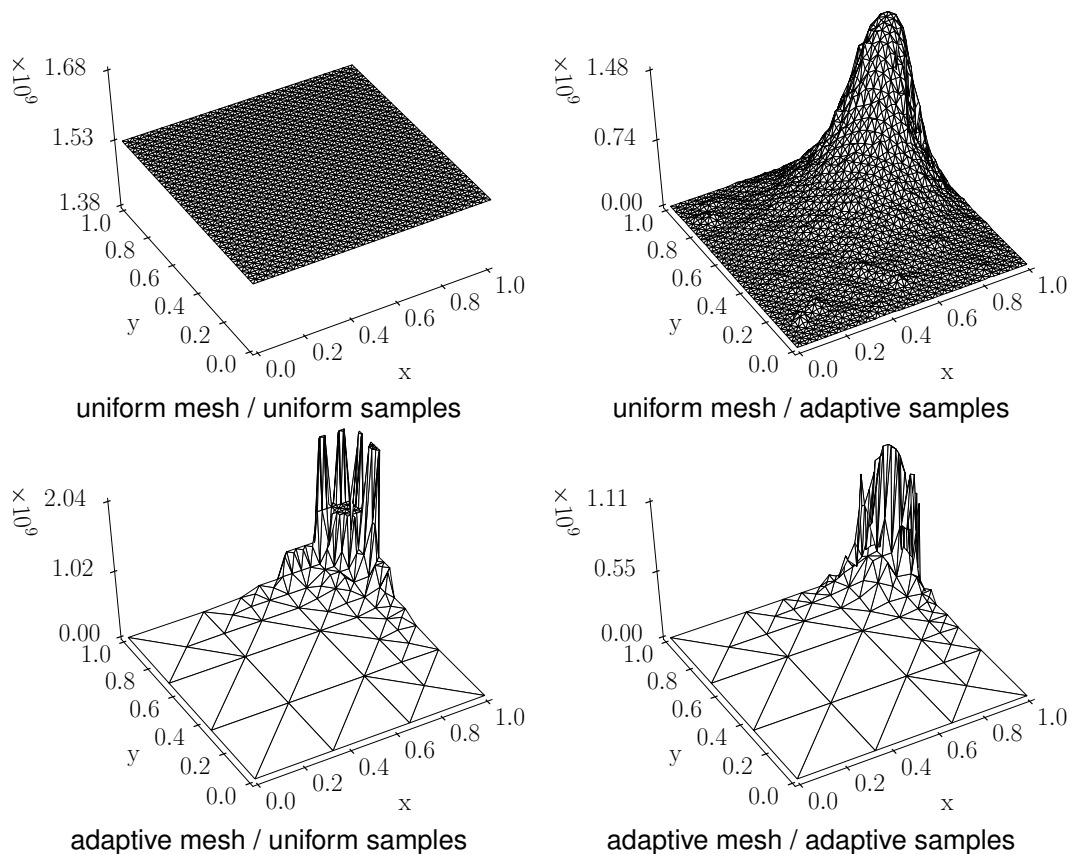


Figure 4: The weighted computational effort \mathcal{C}_T from (20) for each element $T \in \mathcal{T}$ for different methods.

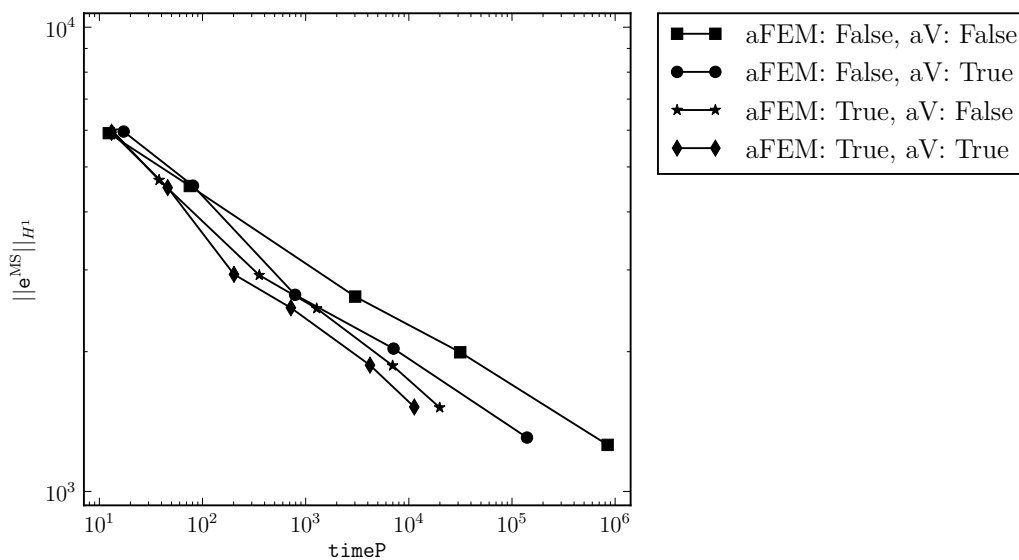


Figure 5: Convergence in the H^1 norm for the different methods. The abbreviations are aFEM for finite element adaptivity and aV for the localized adaptive number of samples.

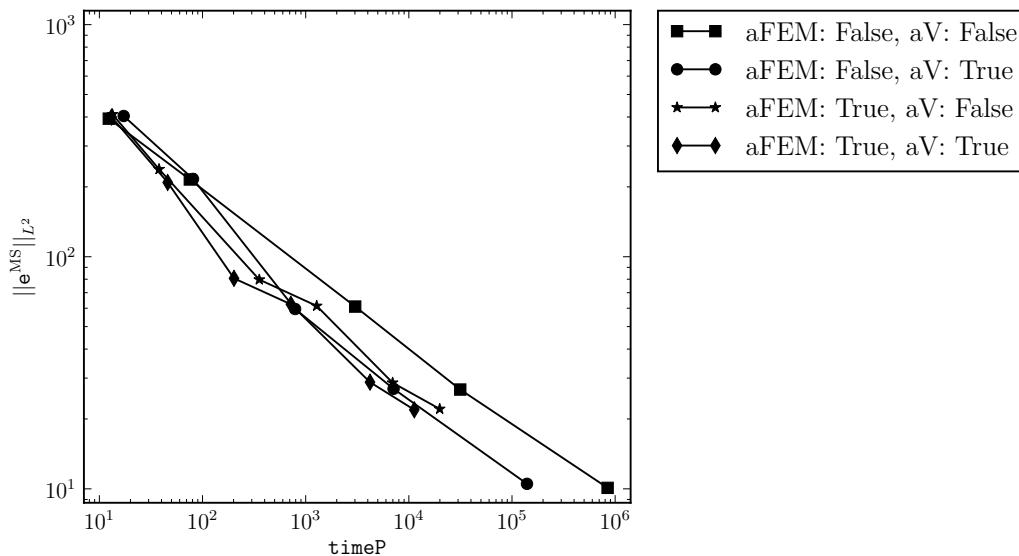


Figure 6: Convergence in the L^2 norm for the different methods. The abbreviations are aFEM for finite element adaptivity and aV for the localized adaptive number of samples.

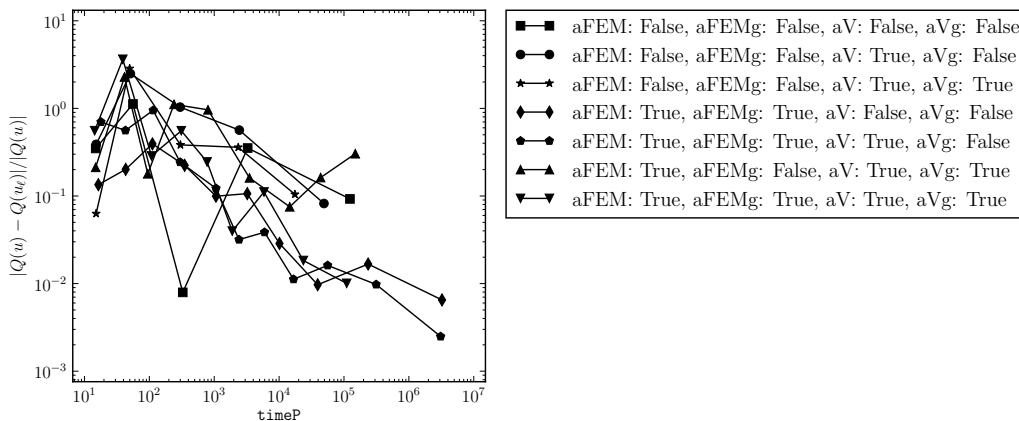


Figure 7: Convergence for the goal error for the different methods. The abbreviations are aFEM for finite element adaptivity, aFEMg for goal-weighted finite element adaptivity, aV for the localized adaptive number of samples and aVg for the goal-weighted localized adaptive number of samples.

- [3] Ivo Babuška, Raúl Tempone, and Georgios E. Zouraris. Galerkin finite element approximations of stochastic elliptic partial differential equations. *SIAM J. Numer. Anal.*, 42(2):800–825, 2004.
- [4] Ivo Babuška, Raúl Tempone, and Georgios E. Zouraris. Solving elliptic boundary value problems with uncertain coefficients by the finite element method: the stochastic formulation. *Comput. Methods Appl. Mech. Engrg.*, 194(12-16):1251–1294, 2005.
- [5] Andrea Barth, Annika Lang, and Christoph Schwab. Multilevel Monte Carlo method for parabolic stochastic partial differential equations. *BIT*, 53(1):3–27, 2013.
- [6] Carsten Carstensen, Martin Eigel, Ronald H.W. Hoppe, and Caroline Löbhard. A review of unified a posteriori finite element error control. *Numer. Math. Theor. Meth. Appl.*, 5(4):509–558, 2012.
- [7] J. Charrier, R. Scheichl, and A. L. Teckentrup. Finite element error analysis of elliptic PDEs with random coefficients and its application to multilevel Monte Carlo methods. *SIAM J. Numer. Anal.*, 51(1):322–352, 2013.
- [8] George Christakos. *Random field models in earth sciences*. Courier Corporation, 2012.
- [9] K. A. Cliffe, M. B. Giles, R. Scheichl, and A. L. Teckentrup. Multilevel Monte Carlo methods and applications to elliptic PDEs with random coefficients. *Comput. Vis. Sci.*, 14(1):3–15, 2011.
- [10] Willy Dörfler. A convergent adaptive algorithm for Poisson’s equation. *SIAM Journal on Numerical Analysis*, 33(3):1106–1124, 1996.
- [11] Martin Eigel, Claude Jeffrey Gittelsohn, Christoph Schwab, and Elmar Zander. Adaptive stochastic Galerkin FEM. *Comput. Methods Appl. Mech. Engrg.*, 270:247–269, 2014.
- [12] Martin Eigel, Christian Merdon, and Johannes Neumann. An adaptive multi level Monte–Carlo method with stochastic bounds for quantities of interest in groundwater flow with uncertain data. *WIAS Preprint*, 2060, 2014.
- [13] Philipp Frauenfelder, Christoph Schwab, and Radu Alexandru Todor. Finite elements for elliptic problems with stochastic coefficients. *Comput. Methods Appl. Mech. Engrg.*, 194(2-5):205–228, 2005.
- [14] Roger G Ghanem and Pol D Spanos. *Stochastic finite elements: a spectral approach*. Courier Corporation, 2003.
- [15] Michael B. Giles. Multilevel Monte Carlo path simulation. *Operations Research*, 56(3):607–617, 2008.
- [16] I. G. Graham, F. Y. Kuo, D. Nuyens, R. Scheichl, and I. H. Sloan. Quasi-Monte Carlo methods for elliptic PDEs with random coefficients and applications. *J. Comput. Phys.*, 230(10):3668–3694, 2011.

- [17] Frances Y. Kuo, Christoph Schwab, and Ian H. Sloan. Quasi-Monte Carlo finite element methods for a class of elliptic partial differential equations with random coefficients. *SIAM J. Numer. Anal.*, 50(6):3351–3374, 2012.
- [18] Olivier P Le Maître and Omar M Knio. *Introduction: Uncertainty Quantification and Propagation*. Springer, 2010.
- [19] Gabriel J Lord, Catherine E Powell, and Tony Shardlow. *An Introduction to Computational Stochastic PDEs*. Number 50. Cambridge University Press, 2014.
- [20] Hermann G. Matthies and Andreas Keese. Galerkin methods for linear and nonlinear elliptic stochastic partial differential equations. *Comput. Methods Appl. Mech. Engrg.*, 194(12-16):1295–1331, 2005.
- [21] G. N. Milstein and M. V. Tretyakov. *Stochastic numerics for mathematical physics*. Scientific Computation. Springer-Verlag, Berlin, 2004.
- [22] Fabio Nobile, Raul Tempone, and Clayton G. Webster. An anisotropic sparse grid stochastic collocation method for partial differential equations with random input data. *SIAM J. Numer. Anal.*, 46(5):2411–2442, 2008.
- [23] Fabio Nobile, Raul Tempone, and Clayton G. Webster. A sparse grid stochastic collocation method for partial differential equations with random input data. *SIAM J. Numer. Anal.*, 46(5):2309–2345, 2008.
- [24] Christoph Schwab and Claude Jeffrey Gittelsohn. Sparse tensor discretizations of high-dimensional parametric and stochastic PDEs. *Acta Numer.*, 20:291–467, 2011.
- [25] Ralph C Smith. *Uncertainty Quantification: Theory, Implementation, and Applications*, volume 12. SIAM, 2013.
- [26] Radu Alexandru Todor and Christoph Schwab. Convergence rates for sparse chaos approximations of elliptic problems with stochastic coefficients. *IMA J. Numer. Anal.*, 27(2):232–261, 2007.